Albumin-Bound Quercetin Repairs Vitamin E Oxidized by Apolipoprotein Radicals in Native HDL_3 and LDL†

Paulo Filipe,[‡,§] Larry K. Patterson,[§,||] David M. Bartels,[||] Gordon L. Hug,[||] João P. Freitas,[‡] Jean-Claude Mazière,[§,⊥,#] René Santus,[▽,○] and Patrice Morlière*[,§,⊥,#]

Faculdade de Medicina de Lisboa, Hospital Santa Maria, Clinica Universitária de Dermatologia, 1600 Lisbon, Portugal, INSERM, ERI12, F-80054 Amiens, France, University of Notre Dame, Radiation Laboratory, Notre Dame, Indiana 46556, Université de Picardie Jules Verne, Faculté de Médecine et de Pharmacie, EA 2087, F-80036 Amiens, France, CHU Amiens Nord, Laboratoire de Biochimie, F-80054 Amiens, France, INSERM, U697, F-75475 Paris, France, and Muséum National d'Histoire Naturelle, Département RDDM, F-75231 Paris, France

Received July 19, 2007; Revised Manuscript Received September 10, 2007

ABSTRACT: In the minor fraction of HDL_3 containing α-tocopherol (αTocOH), selective one-electron oxidation of Trp and Tyr residues of apolipoproteins A-I and A-II by $^{\bullet}Br_2^-$ radical-anions produces the corresponding semioxidized species, $TyrO^{\bullet}$ and $^{\bullet}$Trp. Repair of $TyrO^{\bullet}$ by endogenous αTocOH generates the α-tocopheroxyl radical ($\alpha TocO^{\bullet}$). Fast spectroscopic studies show that two populations representing 80% of $\alpha TocO^{\bullet}$ initially formed are repaired over several seconds with rate constants of 3.0×10^6 and 1.5×10^5 M^{-1} s^{-1} by quercetin bound to human serum albumin (HSA) at physiologically relevant concentration. Formation of HSA-bound quercetin radicals ($^{\bullet}Q_b$) is observed. In the major fraction of HDL_3 particles lacking αTocOH, $TyrO^{\bullet}$ and $^{\bullet}$Trp are repaired by free and HSA-bound quercetin. In LDL particles which all contain αTocOH, $\alpha TocO^{\bullet}$ radicals are formed in the millisecond time scale by repair of $TyrO^{\bullet}$ radicals produced in apolipoprotein B. Then, 75% of initial $\alpha TocO^{\bullet}$ are repaired over seconds by HSA-bound quercetin (rate constant: 2.0×10^6 M^{-1} s^{-1}). HSA-bound quercetin can also repair $^{\bullet}$Trp radicals. In O_2-saturated solutions, the fraction of $\alpha TocO^{\bullet}$ radicals (more than 50%) not repaired by superoxide radical-anions can be repaired by HSA-bound quercetin with formation of $^{\bullet}Q_b$ but to a much lesser extent in LDL than in HDL.

Oxidation of proteins plays a key role in the pathophysiological disturbances observed with some major diseases such as atherosclerosis (*1*) and central nervous system degeneration (*2*). The two aromatic amino acids, Tyr and Trp, as well as Cys are known to be the most oxidizable residues in proteins (*3*). They are readily modified by various initiators of oxidative (*4*) and photo-oxidative (*5*) stresses such as activated oxygen species and other free radicals leading to subsequent loss of protein structure and function. The consequences of protein oxidation may be particularly well illustrated by the atherogenic process. Here, the oxidized apolipoprotein B100 (apoB[1]) is recognized by the unregulated scavenger receptor of macrophages, leading to oxidized LDL accumulation and foam cell formation (*6*). Additionally, the integrity of apolipoprotein A-I (apoAI) of HDL_3 is required for reverse cholesterol transport activity, its primary function, and oxidized HDL_3 loses its ability to promote cholesterol efflux from macrophage foam cells (*7*) and to inhibit LDL oxidation (*8*). It is believed that, *in vivo*, HDL_3 and LDL oxidation occurs within lesions of the artery wall where the NADPH oxidase of the activated phagocytes produces $^{\bullet}O_2^-$ radical-anions and H_2O_2. These reactive oxygen species can subsequently react with redox metal ions present in the locally inflamed area to produce the strongly oxidizing $^{\bullet}$OH radical by Fenton-like reactions or are processed by peroxidases of phagocytes such as myeloperoxidase (MPO) (*9*). Either pathway may produce semioxidized amino acids which act as reactive radical intermediates (*10*). In the case of HDL, the phenoxyl tyrosyl radical ($TyrO^{\bullet}$), produced either by one-electron oxidation of Tyr or by $^{\bullet}$OH addition to its phenoxyl ring, has been reported to produce protein cross-linking through bityrosyl bridges formed by intermolecular radical recombination (*11*). Additionally, Peng *et al.* recently reported that mono- and di-hydroxytryptophan, the end-products of the one-electron oxidation of Trp ($^{\bullet}$Trp) and

† This work was supported by the Franco-Portuguese exchange programs GRICES-INSERM 2005-2006 and Pessoa 07958NF. Notre Dame Radiation Laboratory is supported by the Office of Basic Energy Sciences of the U.S. Department of Energy. This is document 4724 from the Notre Dame Radiation Laboratory.

* To whom correspondence should be addressed: INSERM ERI12, Laboratoire de Biochimie, CHU Amiens Nord, place Victor Pauchet, 80054 Amiens Cedex 1, France; tel, +33 3 22 66 86 69; fax, +33 3 22 66 89 17; e-mail, morliere.patrice@chu-amiens.fr.

‡ Faculdade de Medicina de Lisboa, Clinica Universitária de Dermatologia.

§ INSERM, ERI12.

|| University of Notre Dame, Radiation Laboratory.

⊥ Université de Picardie Jules Verne, Faculté de Médecine et de Pharmacie.

CHU Amiens Nord, Laboratoire de Biochimie.

▽ INSERM, U697.

○ Muséum National d'Histoire Naturelle, Département RDDM.

[1] Abbreviations: αTocOH, α-tocopherol; $\alpha TocO^{\bullet}$, α-tocopheroxyl radical; apoAI, apolipoprotein A-I; apoAII, apolipoprotein A-II; apoB, apolipoprotein B; $^{\bullet}$Trp, semioxidized Trp; $TyrO^{\bullet}$, semioxidized Tyr; QH, quercetin.

10.1021/bi701419d CCC: $37.00
Published on Web 11/16/2007

of •OH addition (*12*), may be involved in the MPO-induced loss of apoAI structure and activity (*13*). In this latter mechanism, the modification of Tyr residues is not involved. In the case of LDL, it has been shown that oxidation of Trp residues of native LDL, induced by Cu^{2+} or by irradiation with UVB light, leads to •Trp formation and initiation of lipid peroxidation as a secondary event (*5*, *14*) and that •Trp radicals may oxidize Tyr residues of LDL to form the TyrO• radical (*15*).

To better understand the roles played by these radicals in the initial stages of the pathologies discussed above, we have recently studied the kinetic and spectral behavior of •Trp and TyrO• radicals generated by the selective $•Br_2^-$ oxidation in the apoAI and apolipoprotein A-II (apoAII) of HDL_3, as well as in the apoB of LDL. These studies were carried out with pulse radiolysis techniques on a time scale extending from tens of microseconds to tens of seconds (*16*). It was observed that the endogenous antioxidant α-tocopherol (αTocOH) of native HDL_3 and LDL partially repairs apoAI damage by reduction of TyrO• radicals but not •Trp radicals. Given the peculiar role attributed to flavonoid-type antioxidants in the control of atherogenesis (*17*), and in light of our preceding work on the repair of apoB radicals of LDL preloaded with a model flavonoid—the flavonol, quercetin (Q) (*15*)—it is of apparent interest to determine whether QH bound to its physiological carrier, human serum albumin (HSA) (*18*), may counterbalance the incomplete repair by endogenous αTocOH of damage to the apolipoproteins of HDL_3 and LDL and ameliorate its subsequent biological consequences. We show here that the fraction of QH bound to HSA can indeed repair the portion of •Trp and TyrO• radicals generated in apoAI, apoAII, and apoB not repairable by αTocOH. It also effectively repairs the αTocO• radicals on a time scale extending over several seconds thereby replenishing αTocOH consumed within the LDL and HDL_3 particles in either the absence or presence of oxygen. To our knowledge, this is the first time that the kinetics for the sequence of molecular mechanisms by which QH acts as an inhibitor of lipoprotein oxidation has been quantified.

EXPERIMENTAL PROCEDURES

Materials. All chemicals were of analytical grade and were used as received from the suppliers. Quercetin and fatty acid free HSA were purchased from Sigma (St. Louis, MO). The 10 mM, pH 7, buffer was prepared with Na and K phosphates from Merck in pure water obtained with a reverse osmosis/deionization system from Serv-A-Pure Co.

Preparation of HDL_3 and LDL. Lipoproteins from pooled plasma of fasting healthy normolipidemic human volunteers were prepared in the presence of 0.5 mM EDTA by sequential ultracentrifugation at 105000*g*. HDL_3 was taken as the 1.125−1.210 density fraction while LDL was isolated in the 1.024−1.060 density fraction (*19*). The LDL and HDL_3 fractions were free of apolipoprotein E. For all pulse radiolysis experiments, EDTA was removed by two cycles of dialysis against 2 L of 10 mM, pH 7, phosphate buffer with 0.1 M KBr at 4 °C beginning 24 h prior to the experiments. HDL_3 concentration was estimated from its protein content on the basis of an average protein content of 2 apoAI and 1.5 apoAII per HDL_3 particle (*20*), *i.e.* ∼ 80,000 g of protein per mole of HDL_3. Absorbance spectra of lipoprotein solutions were recorded before and after pulse radiolysis experiments. Sets of measurements were made in July and again the following March. Freshly isolated lipoproteins, native HDL_3 and LDL, were prepared using blood samples from the same donors for each set, and comparable spectral and kinetics data were obtained. The absence of oxidation during the dialysis of LDL has been discussed in one of our earlier reports (*21*), and there is no reason to believe that this behavior would be different in HDL.

Determination of α-Tocopherol and β-Carotene Contents of HDL_3 and LDL. The simultaneous determination of αTocOH and β-carotene was carried out by reverse phase HPLC using a method derived from several published reports (*22*−*24*). Aliquots of 250 μL of LDL (∼2 mg of proteins) or HDL_3 (∼1.5 mg of proteins) were added to 1 mL of methanol, 250 μL of distilled water, and 25 μL of 1 mM α-tocopherol acetate as internal standard. Then this mixture was vigorously shaken for 30 s. After addition of hexane (2 mL), the solution was vortex-mixed for 1 min, then centrifuged during 10 min at 4,500 rpm. After centrifugation, 1.5 mL of the supernatant was evaporated to dryness under nitrogen. Before HPLC measurement, the dry extract was dissolved in 250 μL of an ethanol/dichloroethane mixture (4:1, v/v). Reverse phase HPLC was carried out with a Bondapak C18/Corasil precolumn (30−50 μm, 2.3 cm × 0.39 cm) and a μBondapak (10 μm, 15 cm × 0.39 cm) provided by Waters. A gradient of two mobile phases (20 min, flow rate: 1 mL/min) was used for elution. Phase A was a mixture of water/acetonitrile/methanol (30:50:20, v/v/v) and phase B a mixture of acetonitrile/methanol/ ethanol/dichloroethane (10:10:50:30, v/v/v/v). Absorbances were monitored at 292 nm (ϵ = 4,070 M^{-1} cm^{-1}) and at 452 nm (ϵ = 137,400 M^{-1} cm^{-1}) to detect αTocOH and β-carotene, respectively.

Fluorometric Determination of the Fraction of Quercetin Bound to HSA in the Presence of Lipoproteins. The fraction of QH bound to HSA after addition of lipoproteins was determined using the fluorometric method described by Dufour and Dangles (*25*). Fluorescence measurements were carried out with a RF-5301 PC SHIMADZU spectrofluorometer. Optical quartz cells (0.5 cm × 0.5 cm) were used in order to minimize inner filter effects due to carotenoid absorbance in the solutions containing both LDL and HSA. Nevertheless, fluorescence intensities were corrected for inner filter effects whenever necessary.

Pulse Radiolysis. The pulse radiolysis system used for kinetic measurements on time scales up to 3−4 ms has been previously described (*26*, *27*). For longer time scales (up to 1 min) the conventional detection system is replaced by an OLIS double-beam rapid scan spectrophotometer which facilitates simultaneous kinetic and spectral measurements at long times. In all experiments, a Corning O-52 optical filter, which removes all wavelengths shorter than 330 nm, was placed in the analyzing light beam preceding the sample cell to avoid apolipoprotein and αTocOH photo-oxidation (*5*). Radical concentrations, calculated from transient absorption data are referenced to $•(SCN)_2^-$ dosimetry (*28*). Radiolytic yield is generally expressed by its *G* value, i.e., the number of radicals generated per 100 eV of absorbed energy. However, such yields, normally expressed in units of grays, may be recast as radical concentrations per unit radiation

Table 1: Concentrations (μM) of Free Quercetin (QH_f), of Quercetin Bound to HSA (QH_b), and of Quercetin Bound to HDL_3 or LDL (QH_b') under Various Experimental Conditions[a]

$[QH_t]^b = [HSA]$ (μM)	$QH_b{}^b +$			$QH_b'{}^b +$		$QH_f +$	
	no lipo-protein	HDL_3	LDL	HDL_3	LDL	HDL_3	LDL
5	2.0	1.0	1.0 (a), 0.45 (b)	2.8	2.8 (a), 4.1 (b)	1.2	1.2 (a), 0.45 (b)
2.5	0.65	0.35		1.35		0.8	

[a] Fluorescence experiments were carried out at room temperature with 18.75 μM HDL_3 or 2.4 μM (a) and 4.8 μM (b) LDL in pH 7 phosphate buffer. Fluorescence measured in 5 × 5 mm optical cells was excited with 450 nm light and read at 528 nm, 15 min after addition of the lipoproteins, but the fluorescence intensity was stabilized after 5 min. [b] $[QH_t]$ is the total quercetin concentration. The QH_b values were obtained with the fluorescence data, and QH_f values were calculated using the mass action law. Hence, QH_b' values were calculated as $[QH_b'] = [QH_t] - [QH_f] - [QH_b]$.

dose (*e.g.* a *G* value of 6.13 corresponds to a concentration of 0.63 μM·kg/J or 0.63 μM/Gy). As a convenience for the general reader, *G* values are expressed hereafter in units of μM/Gy.

Solutions for pulse radiolysis were prepared in 10 mM, pH 7, phosphate buffer and saturated with pure N_2O or O_2 as desired. All solutions contained 0.1 M Br^-, a concentration sufficient to ensure that essentially all $^{\bullet}OH$ are converted to $^{\bullet}Br_2^-$. To avoid lipoprotein denaturation, small volumes (up to 15 mL) of the buffer were first bubbled for 15 min with either pure N_2O or O_2. Aliquots of an equimolar 200 μM HSA−quercetin solution were first added to the buffer, and then 1−2 mL of dialyzed stock lipoprotein solution was added under anaerobic conditions to the N_2O- or O_2-saturated buffer. The resulting solution was further slowly bubbled gently with the desired gas during 5 more minutes prior to pulse radiolysis experiments. Unless otherwise stated, the lipoprotein concentrations in the pulsed solutions were 18.75 μM and 2.4 μM for HDL_3 and LDL, respectively. To minimize the quantity of lipoproteins consumed in each experiment, a microcell (optical path, 1 cm; volume, 400 μL) was used for transient recording. This microcell was emptied and refilled after each shot to ensure that all data were obtained with un-irradiated lipoprotein solutions. Kinetics and spectral measurements were taken twice, and the results were reproducible from day to day. Numerical integrations, for analyses of rate data, were carried out using Scientist software from Micromath Scientific Software. Rate constants have been determined from raw data by the calculations with the above software and show the precision of curve fitting.

RESULTS AND DISCUSSION

Determination of the Fraction of Quercetin Bound to Human Serum Albumin. An equilibrium binding constant of 2.6×10^5 M^{-1} for the binding of QH to HSA in plasma has been reported by Boulton *et al.* (*18*). In our experiments where the concentrations of HDL_3 and LDL exceeded that of HSA, it was necessary to determine the fraction of QH remaining bound to HSA after lipoprotein addition to an equimolar HSA−QH solution. In pH 7 buffer, QH is nonfluorescent. Upon addition of increasing concentration of HSA, the binding of QH to HSA produces an 82% fluorescence quenching of the single Trp 214 of HSA (*29*), and a progressive red-shift in the absorbance maximum occurs
(*30*). Fluorescence is observed in the 490−590 nm range (emission peak at 528 nm) under excitation at 450 nm (*25*). The intensity of this fluorescence reaches a plateau at high $[HSA]/[QH_t]$ ratios, $[QH_t]$ being the total concentration of QH in the solution. The concentration of QH bound to HSA (QH_b) can be estimated at low $[HSA]/[QH_t]$ ratio, knowing the fluorescence intensity at plateau measured with a $[HSA]/[QH_t]$ ratio of 20 where all the QH can be assumed to be bound to HSA. As can be seen in Table 1, QH_b was found to be 2.0 and 0.65 μM respectively for equimolar HSA−QH solutions of 5 and 2.5 μM. The concentrations stated here, 5 and 2.5 μM, are the total concentrations of each component in solution. Assuming a 1:1 HSA−QH complex, these values lead to a binding constant of 2.1×10^5 M^{-1}, which is consistent with literature values (*18*, *30*).

Interestingly, no fluorescence is observed upon addition of 5 μM QH to solutions containing only HDL_3 (18.75 μM) or LDL (2.4 μM), the concentration conditions routinely used in the pulse radiolysis experiments described below. As a result, the concentration of QH remaining bound to HSA in the presence of the lipoproteins can be fluorometrically determined, as detailed above. These values are given in Table 1. In an 18.75 μM HDL_3 containing 5 μM equimolar HSA and QH, it may be seen that about 50% of QH originally bound to HSA in the absence of HDL_3 remains bound. Similarly, it is found that about 50% of the originally HSA bound QH is still bound in the presence of 2.4 μM LDL.

Spectral Evidence for Repair by Quercetin of apoAI, apoAII, and α-Tocopheroxyl Radicals in Native HDL_3. In pulse radiolysis of N_2O-saturated solutions containing 0.1 M Br^-, the $^{\bullet}Br_2^-$ radical-anion is produced with a yield $G = 0.64$ μM/Gy by the reaction

$$^{\bullet}OH + 2Br^- \rightarrow {}^{\bullet}Br_2^- + OH^- \quad (1)$$

The rate constant for eq 1 (*31*) combined with the excess of Br^- as compared to that of LDL assures that less than 0.1% of $^{\bullet}OH$ radicals react directly with LDL.

Recent results from our laboratory (*16*) demonstrate that the fast oxidation of apoAI and apoAII by $^{\bullet}Br_2^-$ may be written

$$^{\bullet}Br_2^- + (\text{apoAI, apoAII}) \rightarrow {}^{\bullet}(\text{apoAI, apoAII}) + 2Br^- + H^+ \quad (2)$$

Analysis of the $TyrO^{\bullet}$ and $^{\bullet}Trp$ radical yields demonstrates that Tyr and Trp residues are the only initial targets of HDL_3 oxidation by $^{\bullet}Br_2^-$ radicals. The transient absorbance spectrum (Figure 1A) shows the characteristic absorbance of these radical species with maxima at 410 nm ($\epsilon = 2{,}700$ M^{-1} cm^{-1})

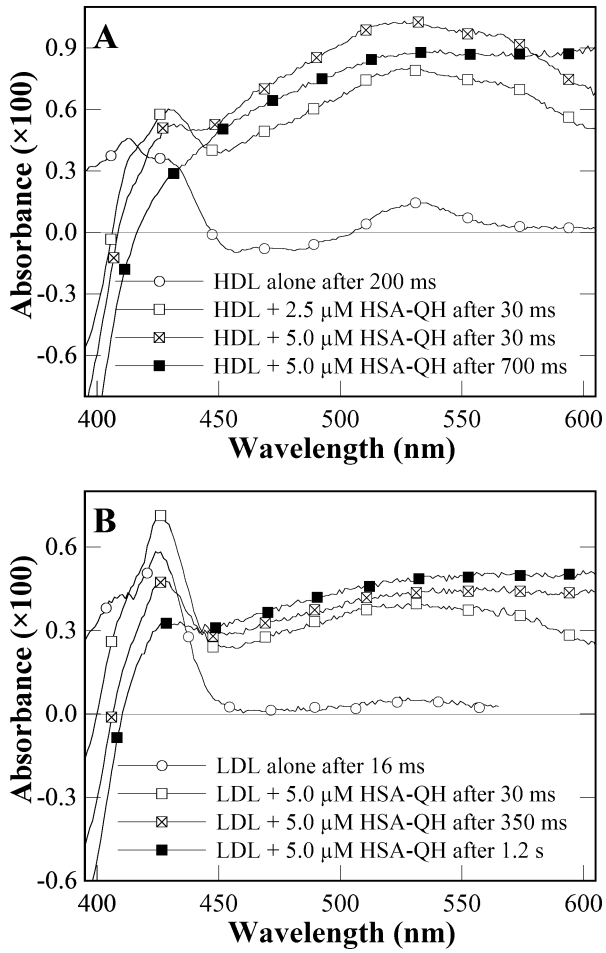

FIGURE 1: A. Absorbance of apolipoprotein and quercetin radicals in HDL_3. (○) Transient absorbance spectra of 12.5 μM HDL_3 in N_2O-saturated 10 mM, pH 7, phosphate buffer containing 0.1 M KBr, recorded 200 ms after oxidation with $^{\bullet}Br_2^-$ radical-anions. Radiolytic dose was 5.1 Gy. (□, × in □, ■) same but solutions contained 18.75 μM HDL_3, 2.5 μM HSA, and 2.5 μM QH (□) or 18.75 μM HDL_3, 5 μM HSA and 5 μM QH (× in □, ■). Spectra were recorded 30 ms (□, × in □) and 700 ms (■) after oxidation with $^{\bullet}Br_2^-$ radical-anions. Radiolytic dose was 4.6 Gy. B. Absorbance of apoB and quercetin radicals in LDL. (○) Transient absorbance spectra of 1.6 μM LDL in N_2O-saturated 10 mM, pH 7, phosphate buffer containing 0.1 M KBr, recorded 16 ms after oxidation with $^{\bullet}Br_2^-$ radical-anions. Radiolytic dose was 6.2 Gy. (□, × in □, ■) same but the solutions contained 2.4 μM LDL, 5 μM HSA, and 5 μM QH. Spectra were recorded 30 ms (□), 350 ms (× in □), and 1.2 s (■) after oxidation with $^{\bullet}Br_2^-$ radical-anions. Radiolytic dose was 5.1 Gy.

and 520 nm (ϵ = 1,750 M^{-1} cm^{-1}) for TyrO$^{\bullet}$ and $^{\bullet}$Trp, respectively. Most $^{\bullet}$Trp radicals disappear within 1 ms, but a small fraction of them, representing one oxidized Trp per particle, decays over seconds (*16*).

The oxidation of Trp and Tyr residues by $^{\bullet}Br_2^-$ radical-anions is followed in the millisecond time domain by a slow and partial intramolecular repair of TyrO$^{\bullet}$ by αTocOH according to the reaction

$$\alpha\text{TocOH} + {}^{\bullet}\text{apoAI}, {}^{\bullet}\text{apoAII} \rightarrow \alpha\text{TocO}^{\bullet} + \text{apoAI, apoAII} \quad (3)$$

with formation of the αTocO$^{\bullet}$ radical (yield: 0.18 μM/Gy) (*16*) identified in Figure 1A by its characteristic absorbance maximum at 430 nm (ϵ = 7,100 M^{-1} cm^{-1}) (*32*). Two percent of αTocO$^{\bullet}$ radicals are in turn repaired by HDL_3 carotenoids (*16*). This behavior explains the bleaching shown in Figure 1A in the 450−500 nm region 0.2 s after the radiolytic pulse. Data in Table 2 illustrate that a majority of native HDL_3 particles constitutively lack αTocOH and carotenoids (*16*). Here, in the two different lipoprotein preparations used in this study, there is, on average, only one αToc molecule for each 3 HDL_3 particles explaining why TyrO$^{\bullet}$ and $^{\bullet}$Trp transient absorbances are still observed 200 ms after HDL_3 oxidation by $^{\bullet}Br_2^-$.

Table 2: Molar Ratio of α-Tocopherol and β-Carotene to Lipoprotein in Several Preparations of Native HDL_3 and LDL Fractions Isolated from Human Plasma of Different Donors by Sequential Ultracentrifugation[a]

antioxidant	HDL_3	LDL
α-tocopherol	0.34, 0.36,[b] 0.31[c]	6.22, 5.84, 5.42, 3.78,[b] 8.75[c]
β-carotene	0.0024, 0.0043,[b] 0.0024[c]	0.28, 0.12, 0.2, 0.11,[b] 0.5[c]

[a] Concentrations were determined by HPLC after extraction as detailed in Experimental Procedures. β-Carotene is used as an indicator of total carotenoid content. [b] Used in pulse radiolysis. [c] Used in fluorescence measurements.

Dramatic changes in the transient absorbance spectrum are observed upon addition of equimolar concentrations of HSA and QH (5 or 2.5 μM) to HDL_3 solution. In the presence of 5 μM QH, for example, the characteristic transient absorbances of TyrO$^{\bullet}$ and αTocO$^{\bullet}$ radicals at about 410 and 430 nm have almost vanished 30 ms after oxidation by $^{\bullet}Br_2^-$ and appear only as shoulders on a broad transient absorbance (Figure 1A). A strong bleaching is observed in the 390−420 nm wavelength region corresponding to the loss of free and HSA-bound QH ground state absorbance. The spectral shape of this transient with a maximum appearing at about 575 nm is consistent with the transient spectrum of semi-oxidized QH species ($^{\bullet}$Q) in the free form published by Jovanovic *et al.* (*33*) in neutral aqueous solutions or as reported in Triton X100 micelles and HSA by Filipe *et al.* (*34*). After 700 ms, the absorbance attributed to free $^{\bullet}$Q species has clearly evolved into another transient spectrum with increased absorbance in the red region, disappearance of the shoulders due to TyrO$^{\bullet}$ and $^{\bullet}$Trp radicals while additional QH bleaching has occurred. Figure 1A also illustrates dependence of spectral evolution on QH concentration since 30 ms after the $^{\bullet}Br_2^-$ oxidation characteristic transient absorbances of the TyrO$^{\bullet}$, αTocO$^{\bullet}$, and $^{\bullet}$Trp radicals appear more clearly affected by the presence of 5 μM QH than by 2.5 μM QH.

Repair of Radicals in Native LDL by Quercetin. Data in Table 2 show that, for the LDL used in these experiments, each LDL particle contains 4 αTocOH molecules. As a consequence, there is a much greater intrinsic probability of reaction (4 to 1) for the repair of TyrO$^{\bullet}$ radicals in LDL as compared to HDL_3 leading to a 10 times faster rate constant for the reaction

$$\alpha\text{TocOH} + {}^{\bullet}\text{apoB} \rightarrow \alpha\text{TocO}^{\bullet} + \text{apoB} \quad (3')$$

in LDL than in HDL_3, the αTocO$^{\bullet}$ yield being 0.12 μM/Gy (*16*). Thus, the TyrO$^{\bullet}$ radical absorbance at 410 nm is rapidly replaced by the αTocO$^{\bullet}$ radical transient absorbance with a maximum at ∼430 nm (Figure 1B). Paradoxically, no carotenoid bleaching is observed in LDL particles despite a much more favorable carotenoid concentration than in HDL_3

(Table 2). It should be noted that direct oxidation of αTocOH by $^{\bullet}Br_2^-$ is unlikely because of the large excess of apoB residues (37 Trp, 9 Cys, 151 Tyr) in LDL available to react with $^{\bullet}Br_2^-$ with rate constants comparable to that of the 4 αTocOH molecules present (e.g., $\sim 10^8$ M^{-1} s^{-1} for free αTocOH).

Upon addition of equimolar (5 μM) HSA and QH, initial transient absorbance changes are observed comparable to those obtained with HDL_3 alone. However, the transient absorbance of the αTocO$^{\bullet}$ radical progressively vanishes and is replaced by the transient spectrum of the free $^{\bullet}$Q radical whose evolution at longer times (Figure 1B) suggests, again, complex radical chemistry in these systems over long durations.

Kinetic Evaluation of the Repair of TyrO$^{\bullet}$, αTocO$^{\bullet}$, and $^{\bullet}$Trp Radicals by Free or Protein-Bound Quercetin in Native HDL_3 and LDL. The HSA and QH concentrations for these experiments have been chosen to conserve valuable lipoproteins while still limiting direct HSA oxidation by the $^{\bullet}Br_2^-$ radical-anions to a level which does not interfere with analysis of kinetics. The rate constant for reaction of $^{\bullet}Br_2^-$ radicals with HDL_3 (*16*), LDL (*15*), HSA (*34*), and QH (*34*, *35*) have been established. Using these values, it may be shown that direct $^{\bullet}Br_2^-$ radical attack on HSA represents only ~10% ([HSA] = 5 μM) and ~5% ([HSA] = 2.5 μM) of that on HDL_3 ([HDL_3] = 18.75 μM). With LDL, the corresponding percentages with [HSA] = 5 μM are ~28% ([LDL] = 2.4 μM) and ~16% ([LDL] = 4.8 μM).

The time dependence of the transient absorbance changes in Figures 1A,B suggests that the formation of $^{\bullet}$Q is due to a series of electron transfer reactions leading to the repair of the TyrO$^{\bullet}$, αTocO$^{\bullet}$, and $^{\bullet}$Trp radicals according to

$$\text{TyrO}^{\bullet} + \text{QH} \xrightarrow{k_{4a}} \text{Tyr} + {}^{\bullet}\text{Q} \quad (4a)$$

$$\alpha\text{TocO}^{\bullet} + \text{QH} \xrightarrow{k_{4b}} \alpha\text{TocOH} + {}^{\bullet}\text{Q} \quad (4b)$$

$$^{\bullet}\text{Trp} + \text{QH} \xrightarrow{k_{4c}} \text{Trp} + {}^{\bullet}\text{Q} \quad (4c)$$

The mass action law applied to the HDL_3 (or LDL), HSA, and QH equilibria demonstrates that, in addition to unbound HSA and HDL_3 (or LDL) molecules, three different QH species coexist in these systems: unbound QH molecules moving freely in the buffer (QH_f), QH bound to HSA (QH_b), and QH bound to HDL_3 (or LDL) (QH_b'). As a result, the repair of the TyrO$^{\bullet}$, αTocO$^{\bullet}$, and $^{\bullet}$Trp radicals may occur from these three QH species. Data in Table 1 show that more than 85% of the HDL_3 particles are free of QH but, depending on the LDL concentration, all the LDL particles may attach a QH molecule.

It is known from our previous study on the repair of oxidative damage to small molecules or peptides by HSA-bound QH (*34*) and repair of damage to apoB of LDL loaded with QH (*15*) that the time scales of the reactions depicted by eqs 4 differ significantly from one another. The repair of TyrO$^{\bullet}$ and $^{\bullet}$Trp in micelles by free QH occurs by fast diffusion controlled bimolecular reactions with rate constants of k_{4a} and $k_{4c} \sim 10^8$ M^{-1} s^{-1} (*34*). Consequently, under our experimental conditions where the concentration of free QH is ~1 μM, the half-time for these reactions would be ~5 ms. The intramolecular repair of HSA radicals by HSA-bound QH is a first-order process taking place within less than 2 ms after oxidation by $^{\bullet}Br_2^-$ radicals (*34*). The intramolecular repair of oxidative damage to apoAI and apoAII by HDL-bound QH and to apoB by LDL-bound QH is expected to take place on the millisecond time scale by reference to our previous work on LDL preloaded with QH. There, the repair of $^{\bullet}$apoB by QH occurs with a rate constant of $\sim 2 \times 10^3$ s^{-1} (*15*). On the other hand, a slow bimolecular repair of apoAI, apoAII, or apoB damage by HSA-bound QH is expected since QH binds to a relatively inaccessible region of domain IIa of HSA leading to slow rates of reaction even with small molecules moving freely in buffer (see ref (*34*) for examples illustrating such an inaccessibility). As a result, complex kinetics reflecting these different reactivities are expected. Such behavior is evident in Figure 2A with HDL_3 and Figure 2B with LDL at the wavelengths of maximum absorbance for the TyrO$^{\bullet}$, αTocO$^{\bullet}$, and $^{\bullet}$Trp radicals and at 390 nm where the absorbance change is mainly due to QH consumption. Consistent with different reactivities of the TyrO$^{\bullet}$, αTocO$^{\bullet}$, and $^{\bullet}$Trp toward the various QH species, it is observed that the bleaching of QH exhibits at least two mechanisms. A fast step occurring on an about 10 ms time scale may be attributed to repair of radicals by free QH or QH bound to lipoproteins (QH_b' in Table 1) whereas a much slower consumption is observed over the 3 s time scale (Figures 2A,B). The kinetic data in Figure 2A suggest different rates of reaction for TyrO$^{\bullet}$, αTocO$^{\bullet}$, and $^{\bullet}$Trp radicals, the slowest being observed for αTocO$^{\bullet}$. This is consistent with αTocOH being less solvent exposed since it resides predominantly at the water−lipid interface, the chromanol moiety of αTocOH interacting with the phospholipid headgroups while the phytyl side chain anchors αTocOH in the lipid monolayer and reduces its mobility (*36*).

Figure 2C shows the $^{\bullet}$Trp transient absorbance change at 520 nm in HDL_3 over a 2 s period with and without added HSA−QH solution. It can be seen that in the absence of QH, the $^{\bullet}$Trp transient absorbance slowly decays over 2 s. In the presence of 2.5 or 5 μM equimolar HSA−QH the fast initial increase in absorbance at this wavelength can be attributed to the fast reaction of free QH or lipoprotein-bound QH with the TyrO$^{\bullet}$, αTocO$^{\bullet}$, and $^{\bullet}$Trp radicals, according to eq 4(a,b,c). This leads to the formation of the strongly absorbing free $^{\bullet}$Q species ($\epsilon \sim 7{,}000$ M^{-1} cm^{-1} at 520 nm (*33*)) within 10 ms (see above). The subsequent absorbance decay on the 0.5 s time scale is clearly QH concentration dependent. Hence, one may reasonably attribute this behavior to the slow repair of the $^{\bullet}$Trp radicals by HSA-bound QH. It can be seen in Figure 2C that the disappearance of transient absorbance during this step corresponds closely to that of the $^{\bullet}$Trp radicals obtained under similar irradiation dose conditions in the absence of QH. This suggests essentially full repair of these long-lived $^{\bullet}$Trp radicals by HSA-bound QH.

An essential function of αTocOH is to impede the initiation and propagation of the harmful radical induced lipid peroxidation in lipoproteins. Hence, the restoration of αTocOH that may be consumed by repair of apolipoprotein damage would bring additional protection to lipoprotein lipids. In this regard, *in vitro* studies have shown (*33*) that, at pH 7, QH can restitute vitamin E, as the redox potentials (E_0($^{\bullet}$Q,H^+/QH) = 0.33 V), and (E_0 (αTocO$^{\bullet}$,H^+/αTocOH) = 0.48 V) favor the electron transfer involved. The repair of αTocO$^{\bullet}$ by HSA-bound QH is particularly relevant to

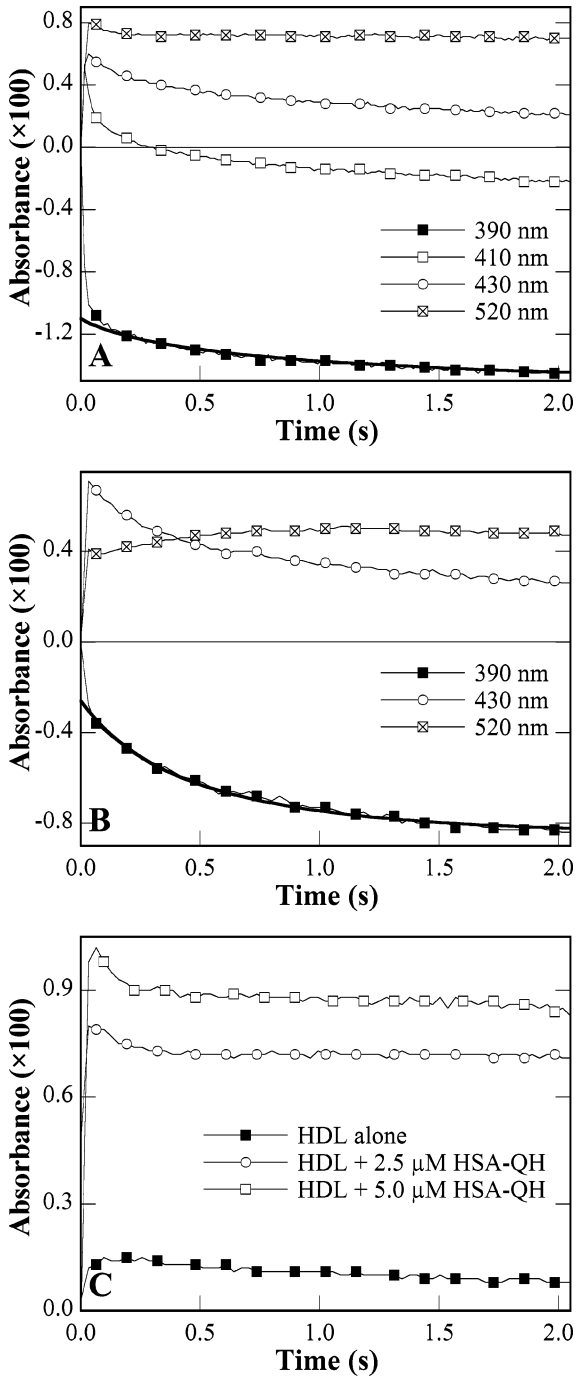

FIGURE 2: A. Kinetics of radical decays in HDL_3. Decay of transient absorbance at 390 nm (■), 410 nm (□), 430 nm (○), and 520 nm (× in □) after pulse radiolysis of 18.75 μM HDL_3 in N_2O-saturated 10 mM, pH 7, phosphate buffer containing 0.1 M KBr, 2.5 μM HSA, and 2.5 μM QH. Radiolytic doses was 4.6 Gy. B. Kinetics of radical decays in LDL. Decay of transient absorbance at 390 nm (■), 430 nm (○), and 520 nm (× in □) after pulse radiolysis of 2.4 μM LDL in N_2O-saturated 10 mM, pH 7, phosphate buffer containing 0.1 M KBr, 5 μM HSA, and 5 μM QH. Radiolytic dose was 5.1 Gy. In both 2A and 2B, the fit with rate equations given in the text is shown by a thick solid line for the transient absorbance change at 390 nm. Starting point for fitting = 0.15 s, coefficient of determination = 0.903 (2A) and 0.986 (2B). C. Kinetics of tryptophan radical decay in HDL_3. Decay of transient absorbance at 520 nm after pulse radiolysis of 12.5 μM HDL_3 in N_2O-saturated 10 mM, pH 7, phosphate buffer containing 0.1 M KBr (■) (radiolytic dose: 5.1 Gy) and of 18.75 μM HDL_3 in N_2O-saturated 10 mM, pH 7, phosphate buffer containing 0.1 M KBr, 2.5 μM HSA, and 2.5 μM QH (○) or 5 μM HSA and 5 μM QH (□) (radiolytic dose: 4.6 Gy).

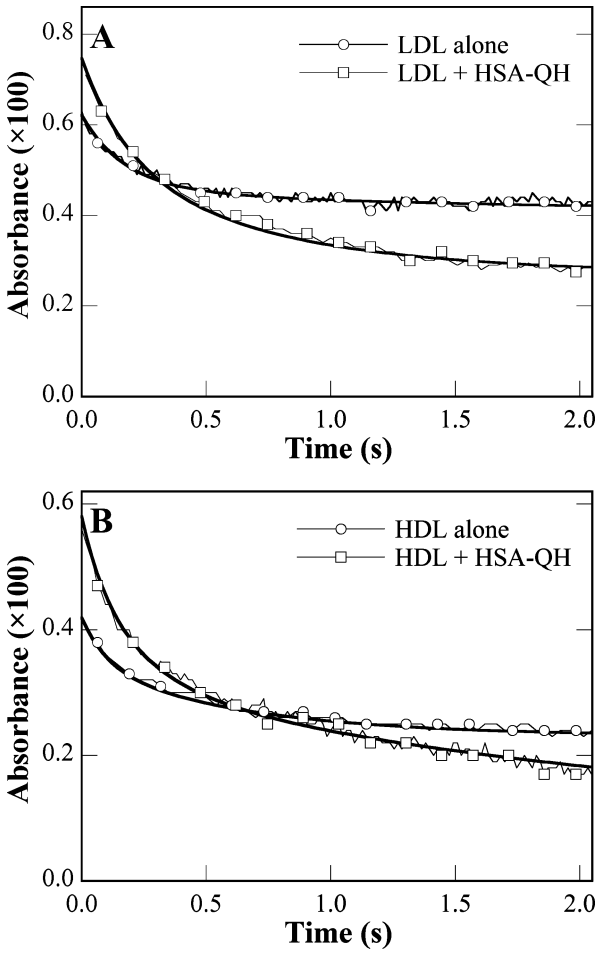

FIGURE 3: A. Kinetics of α-tocopheroxyl radical decay in LDL. Decay of transient absorbance at 430 nm after pulse radiolysis of 1.8 μM LDL in N_2O-saturated 10 mM, pH 7, phosphate buffer containing 0.1 M KBr (○) (dose: 6.2 Gy) or 2.4 μM LDL plus 5 μM HSA and 5 μM QH (□) (dose: 5.1 Gy). B. Kinetics of α-tocopheroxyl radical decay in HDL_3. Decay of transient absorbance at 430 nm after pulse radiolysis of 12.5 μM HDL_3 in N_2O-saturated 10 mM, pH 7, phosphate buffer containing 0.1 M KBr (○) (dose: 5.1 Gy) or 18.75 μM HDL_3 plus 5 μM HSA and 5 μM QH (□) (dose: 4.6 Gy). For both 3A and 3B, the thick solid line shows the fits of decays using the rate equations given in the text. Starting point for fitting = 0 s, coefficient of determination = 0.950 (3A, ○), 0.983 (3A, □), 0.974 (3B, ○), and 0.944 (3B, □).

physiological systems since more than 94% of QH (*18*) or its metabolites (*30*) are bound to HSA in plasma. In humans, the main conjugates resulting from QH metabolism are glucuronides, sulfates, and the 3′-O-methyl derivative (*37*, *38*). It has been shown that they retain antioxidant activity comparable or superior to that of QH (*38*, *39*). Since thermodynamic data are available only for the HSA−QH complex formation, it is therefore a good model to study αTocO• repair attributable to HSA-bound flavonols and to assess the kinetic parameters of such processes.

In Figures 3A,B the decays of the transient absorbance at 430 nm are shown for the αTocO• radical resulting from the repair of amino acid radicals of apoAI, apoAII, and B in the absence or in the presence of a buffered solution of QH and HSA. It can be seen that in the presence of HSA and QH the apparent decay of the αTocO• radical continues over a time scale of several seconds. This increased decay may be attributed to the participation of reaction 4 which in turn involves simultaneous bleaching of ground state QH absor-

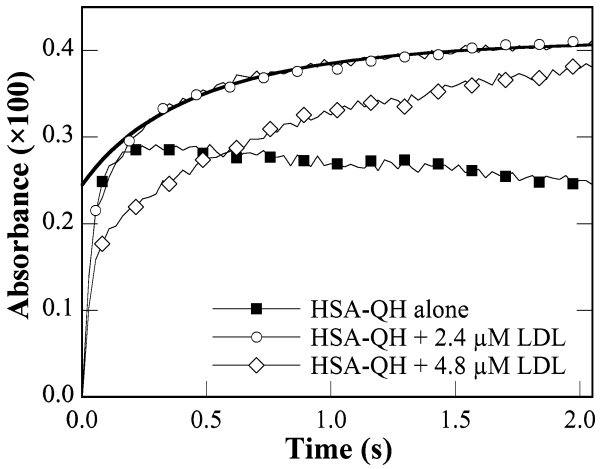

FIGURE 4: Kinetics of quercetin radical formation. Transient absorbance change at 620 nm after pulse radiolysis of 5 μM HSA in N_2O-saturated 10 mM, pH 7, phosphate buffer containing 0.1 M KBr and 5 μM QH (■) (radiolytic dose: 4.6 Gy) or after pulse radiolysis of 5 μM HSA and 5 μM QH in N_2O-saturated 10 mM, pH 7, phosphate buffer containing 0.1 M KBr and 2.4 μM LDL (◇) or 4.8 μM LDL (○) (radiolytic dose: 4.6 Gy). The thick solid line shows the fit of the absorbance change using the rate equation given in the text. Starting point for fitting = 0.15 s, coefficient of determination = 0.964.

bance and formation of the semioxidized QH species. It may be suggested that such formation of the HSA-bound •Q radical species (•Qb) via reaction 4b is responsible for the corresponding changes in the spectral shape of transient absorbance observed on a long time scale with both HDL_3 and LDL (Figures 1A,B). Since the ground state absorbance of QH_b undergoes a large red-shift as compared to free QH, it is likely that the •Qb radical absorbance will differ from that of •Q radical species in the free form.

Kinetics measured at 620 nm (Figure 4), where the only absorbing species are •Q (*15*, *33*) in free form and •Qb, demonstrate the bimolecular nature of this formation. Doubling the LDL concentration from 2.4 to 4.8 μM LDL reduces the HSA-bound [QH_b] from 1.0 to 0.45 μM (Table 1) but increases the LDL-bound [QH_b'] to 4.1 μM. This leads to a much slower •Qb formation, though same final [•Qb], is reached under the same initial $•Br_2^-$ concentration. Additionally, formation and decay kinetics of the •Q radicals generated in the HSA−QH complex in the absence of lipoproteins are included in Figure 4. It is observed that their contribution to the overall kinetics is insignificant as explained at the beginning of the kinetic study discussion.

With the assumption that the kinetics of the reactions observed on a 3 s time scale are solely due to the fraction of QH bound to HSA, the rate equations that must be taken into account for analyzing the repair of αTocO• by HSA-bound QH include not only eq (4b) but also the decay of αTocO• radicals alone after repair of apoB or apo-AI, apo-AII damage by endogenous αTocOH. It has previously been shown (see Table 2 in ref (*16*)) that, in N_2O-saturated solutions, a fraction of αTocO• decays on this time scale by two parallel first-order reactions, according to

$$\alpha\text{TocO}^\bullet \xrightarrow{k_{5a},\, k_{5b}} \text{products} \qquad (5a,b)$$

With LDL alone, a fit of data with $k_{5a} = 5.8\ s^{-1}$ and $k_{5b} = 0.8\ s^{-1}$ (*16*) (Figure 3A) shows that about 67% of the initial αTocO• radicals (population $\alpha\text{TocO}^\bullet_c$) do not disappear whereas about 25% and 8% of the αTocO• radicals (populations $\alpha\text{TocO}^\bullet_a$ and $\alpha\text{TocO}^\bullet_b$ respectively) react *via* the fast and the slow reactions 5a and 5b, respectively.

It may be suggested that these three different populations of αTocO• radicals can be repaired by HSA-bound QH according to the bimolecular reaction path 4b. However, reaction 4b will also be in competition with reaction 5a and 5b. Hence, the rate equations can be written as

$$-\text{d}[\alpha\text{TocO}^\bullet_a]/\text{d}t = (k_{5a} + k_{4b}[\text{QH}_b])[\alpha\text{TocO}^\bullet_a]$$

$$-\text{d}[\alpha\text{TocO}^\bullet_b]/\text{d}t = (k_{5b} + k_{4b}[\text{QH}_b])[\alpha\text{TocO}^\bullet_b]$$

$$-\text{d}[\alpha\text{TocO}^\bullet_c]/\text{d}t = k_{4b}[\text{QH}_b][\alpha\text{TocO}^\bullet_c]$$

$$-\text{d}[\text{QH}_b]/\text{d}t = k_{4b}[\text{QH}_b]([\alpha\text{TocO}^\bullet_a] + [\alpha\text{TocO}^\bullet_b] + [\alpha\text{TocO}^\bullet_c])$$

where $\alpha\text{TocO}^\bullet_a$, $\alpha\text{TocO}^\bullet_b$, and $\alpha\text{TocO}^\bullet_c$ are the different αTocO• populations reacting in parallel *via* reactions 5a, 5b, and 4b. A radiolytic dose of 4.6 Gy produces an initial αTocO• concentration ($[\alpha\text{TocO}^\bullet]_{initial}$) of 0.55 μM. As a consequence, $[\alpha\text{TocO}^\bullet_a]_{initial} = 0.25\,[\alpha\text{TocO}^\bullet]_{initial}$, $[\alpha\text{TocO}^\bullet_b]_{initial} = 0.08\,[\alpha\text{TocO}^\bullet]_{initial}$, $[\alpha\text{TocO}^\bullet_c]_{initial} = 0.67\,[\alpha\text{TocO}^\bullet]_{initial}$. The absorbance change at 430 nm is due to the consumption of αTocO• radicals ($\epsilon = 7{,}100\ M^{-1}\ cm^{-1}$), to the formation of •Qb radicals, and to the disappearance of QH_b whose ϵ is $10{,}200\ M^{-1}\ cm^{-1}$ at 430 nm (measured in our laboratory). Contributions from other radicals to the absorbance at this wavelength are negligible since in LDL most TyrO• radicals are rapidly repaired by αTocOH. The quite small •Trp concentration and the molar extinction coefficient of $560\ M^{-1}\ cm^{-1}$ ensure that this radical does not interfere with the kinetic analysis (see Figure 1B in the absence of QH and Figure 2B). The long-lived •Q radicals in the free form are only produced within 10 ms of the radiolytic pulse (see above). At neutral pH, they decay within a few milliseconds to form a stable product by a simple bimolecular reaction (*34*). The excellent fit of the decay (Figure 3A) obtained with $k_{4b} = 2.0 \times 10^6\ M^{-1}\ s^{-1}$ yields a molar absorbance of $8{,}800\ M^{-1}\ cm^{-1}$ at 430 nm for the •Qb radicals. It also suggests negligible contribution of the $\alpha\text{TocO}^\bullet_a$ population to the •Qb radical formation probably because the fast reaction 5a overcomes the repair by QH_b (reaction 4b). On the other hand, the much longer lived $\alpha\text{TocO}^\bullet_b$ population can react fully with QH_b. Overall, it may be concluded that about 75% of the αTocO• radicals are repaired by HSA-bound QH.

If valid, this kinetic scheme must be able to fit data obtained at other wavelengths of interest. At 620 nm, where free •Q and •Qb radicals are the only absorbing species, the slow portion of the absorbance growth is governed by the rate equation

$$\text{d}[\text{•Qb}]/\text{d}t = k_{4b}[\text{QH}_b]([\alpha\text{TocO}^\bullet_b] + [\alpha\text{TocO}^\bullet_c])$$

An excellent fit is obtained with a value of k_{4b} ($2.1 \times 10^6\ M^{-1}\ s^{-1}$) similar to that determined above and allows an estimate of $4{,}000\ M^{-1}\ cm^{-1}$ for the molar absorbance of •Qb radicals at this wavelength (Figure 4). Likewise, at 390 nm the overall negative absorbance is due to consumption

of QH_b (ϵ = 14,400 M^{-1} cm^{-1} at 390 nm, unpublished observation), to the disappearance of αTocO$^\bullet$ (ϵ = 2,200 M^{-1} cm^{-1} at 390 nm (*40*)), and to the formation of $^\bullet$Qb. As above, Trp makes no significant contribution to the kinetic analysis as the molar extinction coefficient at this wavelength is only 630 M^{-1} cm^{-1}. Again an excellent fit is obtained with $k_{4b} = 2.0 \times 10^6$ M^{-1} s^{-1} yielding an estimate of 4,500 M^{-1} cm^{-1} for the molar absorbance of $^\bullet$Qb at 390 nm.

In HDL_3 alone, it is observed (Figure 3B) that 19% of the αTocO$^\bullet$ radicals (the so-called αTocO$^\bullet_a$ population by analogy with LDL) and 26% of the αTocO$^\bullet$ radicals (called the αTocO$^\bullet_b$ population) decay with $k_{5a} = 9.5$ s^{-1} and $k_{5b} = 1.5$ s^{-1}, respectively (*16*). Furthermore, it may be concluded that most of the fraction of TyrO$^\bullet$ and $^\bullet$Trp radicals non repairable by αTocOH in HDL_3 have reacted with QH in the free form (see above and Figures 2A,2C). The same rate equations as those described with LDL were applied to HDL_3 for the repair of the αTocO$^\bullet$ radicals by HSA-bound QH. To this end, the resolution of the rate equations was performed with the same molar absorbance as that determined at 390, 430, and 620 nm with LDL. Figure 3B and Figure 2A illustrate the excellent fits obtained at 430 and 390 nm for the case of a solution of 18.75 μM HDL_3 containing 5 μM HSA and 5 μM QH (430 nm) or containing 2.5 μM HSA and 2.5 μM QH (390 nm). The calculation suggests that, as in LDL, the αTocO$^\bullet_a$ population is also nonrepairable by QH_b probably because the preponderant reaction path is the fast reaction 5a. The calculation also indicates that the αTocO$^\bullet_b$ and αTocO$^\bullet_c$ populations representing 81% of the initially formed αTocO$^\bullet$ are repaired by QH_b with two differing rate constants. Values of $k_{4b} = 3.0 \times 10^6$ M^{-1} s^{-1} and $k_{4b'} = 1.5 \times 10^5$ M^{-1} s^{-1} are determined for the αTocO$^\bullet_b$ and αTocO$^\bullet_c$ populations, respectively. Remarkably enough an excellent fit of the data at 390 nm (i.e., with 2.5 μM HSA and 2.5 μM Q) is obtained using a QH_b concentration of 0.45 μM instead of the experimentally found 0.35 μM (see Table 1) which strongly supports our kinetic model. The fact that in HDL_3 two reaction paths may operate in the repair of the αTocO$^\bullet_b$ and αTocO$^\bullet_c$ populations by QH_b as opposed to a single pathway in LDL is most probably explainable by the large structural differences between the LDL and HDL_3 particles. All LDL particles (diameter ~20 nm) are enveloped by a single apoB. By contrast, the apoprotein content of HDL_3 particles (diameter: 9 nm) is not uniform. The majority of them (~75%) are wrapped with two apoAI and two apoAII while the rest only contains two apoAI. This heterogeneity may render the phospholipid monolayer, where the αTocOH molecules are located, more or less accessible to the HSA-bound QH.

Effect of $^\bullet O_2^-$ on the Consumption of Quercetin in Repair Reactions after Oxidative Damage to Apolipoproteins of LDL and HDL. The processes described above have been characterized under anoxic conditions, precluding any participation from O_2. Because of the obvious relationship to *in vivo* conditions the effects of oxygen on reactions involved in the sequence of mechanisms discussed above have been investigated under aerobic conditions. Pulse radiolysis of an O_2-saturated solution containing 0.1 M Br^- produces $^\bullet O_2^-$ with a radiolytic yield G = 0.34 μM/Gy by the following reactions:

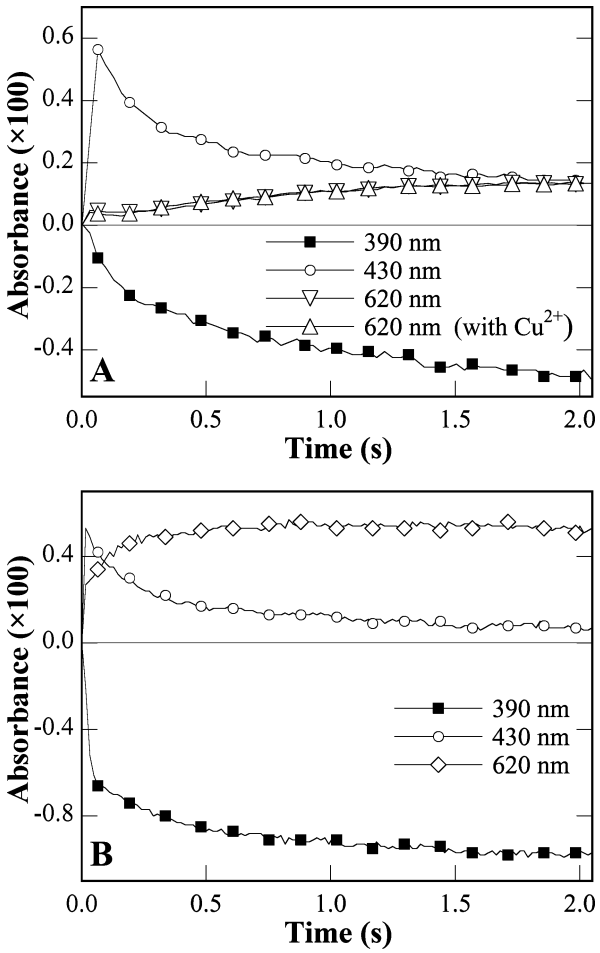

FIGURE 5: A. Kinetics of radical formation and decay in LDL. Decays of transient absorbance at 390 nm (■), 430 nm (○) and increase in absorbance at 620 nm (▽, △) after pulse radiolysis of 2.4 μM LDL in O_2-saturated 10 mM, pH 7, phosphate buffer containing 0.1 M KBr, 5 μM HSA, and 5 μM QH (▽) and 5 μM Cu^{2+} (△). Radiolytic dose was 7.2 Gy. B. Kinetics of radical formation and decay in HDL_3. Decays of transient absorbance at 390 nm (■), 430 nm (○) and increase in absorbance at 620 nm (◇) after pulse radiolysis of 18.75 μM HDL_3 in O_2-saturated 10 mM, pH 7, phosphate buffer containing 0.1 M KBr, 5 μM HSA, and 5 μM QH. Radiolytic dose was 6.6 Gy.

$$e_{aq} + O_2 \rightarrow {}^\bullet O_2^- \quad (6)$$

$$H^\bullet + O_2 \rightarrow {}^\bullet O_2^- + H^+ \quad (7)$$

The radiolytic yield of the $^\bullet Br_2^-$ radicals formed according to eq 1 is reduced to 0.32 μM/Gy. It has been demonstrated that the $^\bullet$Trp and TyrO$^\bullet$ radicals of apoAI, apoAII, and apoB are insensitive to $^\bullet O_2^-$ radical-anions (*16*). In these experiments interference from transition metal ions via Fenton-like reactions is not an issue as shown by data in Figure 5A (see below). Although it is known that ferrous ions can initiate LDL oxidation when incubated with various cells (e.g., smooth muscle cells), it has been shown that ferrous ion initiation in isolated LDL is very inefficient (*41*). Additionally, Janisch *et al.* have recently shown that HSA, in the quantities used here, will displace any copper ions bound to LDL (*39*). The $^\bullet O_2^-$ radical-anion does not react with αTocOH (*32*) but can directly oxidize QH by hydrogen abstraction or electron transfer followed by deprotonation with a rate constant $k_8 = 8 \times 10^5$ M^{-1} s^{-1} (*33*, *34*) according to

$$QH + {}^{\bullet}O_2^- + H^+ \xrightarrow{k_8} {}^{\bullet}Q + H_2O_2 \qquad (8)$$

In the present study, the shapes of transient absorbance spectra (data not shown) observed 30 ms after $^{\bullet}Br_2^-$ oxidation of the HDL_3 and LDL in O_2-saturated solutions containing 5 μM QH and HSA are similar to those shown in Figures 1A,B.

Among the three categories of αTocO$^{\bullet}$ species that have been identified in the lipoproteins (*16*), only two of them react with $^{\bullet}O_2^-$ presumably by the repair reaction

$$\alpha\text{TocO}^{\bullet} + {}^{\bullet}O_2^- + H^+ \rightarrow \alpha\text{TocOH} + O_2 \qquad (9)$$

leading to partial αTocOH restoration. By contrast the proportion of αTocO$^{\bullet}$ species (more than 50%) which, in the absence of QH, is stable over a 3 s time scale (Figures 3A,B) is hardly affected by the presence of $^{\bullet}O_2^-$ radical-anions (*16*).

Figures 5A,B demonstrate that the repair reactions leading to QH oxidation are quite different in HDL_3 and LDL under O_2-saturation. The rate of QH bleaching at 390 nm is much slower in LDL (Figure 5A) than in HDL_3 (Figure 5B) solutions where two distinct steps are clearly observed, as was also observed under N_2O. It is also observed that the extent of $^{\bullet}$Qb formation *via* reaction 4, followed at 620 nm on a 3 s time scale—independent of the presence or absence of 5 μM Cu^{2+}—is markedly inhibited in LDL but is substantial in HDL_3. It should be noted that although very similar initial yields of αTocO$^{\bullet}$ are obtained in HDL_3 and LDL (*e.g.*, ~0.1 μM/Gy), the total apparent yield of QH bleaching in HDL_3 is almost double that observed in LDL.

These observations can be rationalized on the basis of the different αTocOH contents of HDL_3 and LDL; the repair of $^{\bullet}$Trp and TyrO$^{\bullet}$ radicals by αTocOH is not possible in all particles since a majority of them lack αTocOH (see ref (*16*) and Table 2). As a consequence $^{\bullet}$Trp and TyrO$^{\bullet}$ radicals can be directly repaired by QH according to reactions 4a and 4c as previously seen in Figures 1A and 2A while partial repair of αTocO$^{\bullet}$ by $^{\bullet}O_2^-$ observed at 430 nm on Figure 5B is only effective in the minor fraction of HDL_3 particles containing αTocOH. By analogy with observations made in N_2O-saturated solutions, the rapid QH bleaching observed at 390 nm probably involves direct repair of the more solvent exposed TyrO$^{\bullet}$ and $^{\bullet}$Trp formed in apoAI, apoAII by free or bound QH. However, the population of more than 50% of αTocO$^{\bullet}$ radicals, insensitive to $^{\bullet}O_2^-$, may be repaired by HSA-bound QH on the longer 3 s time scale after the $^{\bullet}O_2^-$ radical-anions have disappeared by reaction with αTocO$^{\bullet}$ or with QH or by dismutation. In this regard, the kinetics of QH bleaching observed at 390 nm on the second time scale are similar for the two lipoproteins. This is also consistent with the repair of that portion of αTocO$^{\bullet}$ radicals insensitive to $^{\bullet}O_2^-$. Moreover, the fractions of HSA-bound QH bleached during this slow repair are rather similar (e.g., ~0.25 and 0.35 μM for HDL_3 and LDL, respectively) as estimated from the level of negative absorbance measured 2.5 s after $^{\bullet}Br_2^-$ oxidation. These values which correspond to about half of the initial αTocO$^{\bullet}$ concentration support the above considerations.

CONCLUSIONS

Previous studies of LDL as well as recent work on HDL_3 (*7*, *13*) have shown that not only oxidation of Lys but also oxidation of Tyr and Trp residues are involved in the loss of apoAI and apoB function and in the triggering of lipid peroxidation (*5*, *14*, *42*). In the case of HDL_3, the constitutive lack of αTocOH in a majority of particles (*16*) and the presence of only one αTocOH molecule in the rest may well be a determining factor in triggering the destructive lipid peroxidation. The antioxidant potential of flavonoids has been mostly addressed in terms of lipid peroxidation inhibition (*43*), which occurs on a time scale much longer than that of the present study. For example, Mayer *et al.* have recently studied the efficacy of quercetin and rutin as antioxidants to protect plasma against peroxidation over a period of hours. They determined that quercetin, in conjunction with vitamin E, inhibited oxidative damage to lipoproteins while rutin and vitamin C protected other plasma proteins (*44*). Here, QH has been used as model to elucidate the initial kinetics of two additional mechanisms by which an antiatherogenic effect of flavonoids may operate. All the repair reactions involving HSA-bound QH and lipoproteins are summarized by the scheme given in Figure 6. First, when bound to HSA, their normal physiological state, flavonoids may partly restitute αTocOH, making it available for enhanced protection of HDL_3 and LDL particles against lipid peroxidation. In this regard, it is worthy of note that the HSA-bound QH concentrations used in this work are relevant to those that may be normally found in human plasma for major QH metabolites which retain significant antioxidant activity. Second, our data suggest that bound flavonoids can repair amino acid radicals of apolipoproteins, a most important mechanism with respect to HDL_3 where for physiological reasons a majority of apoAI and apoAII radicals cannot be repaired by αTocOH. Finally, these studies clearly demonstrate that the pulse radiolysis technique, properly applied,

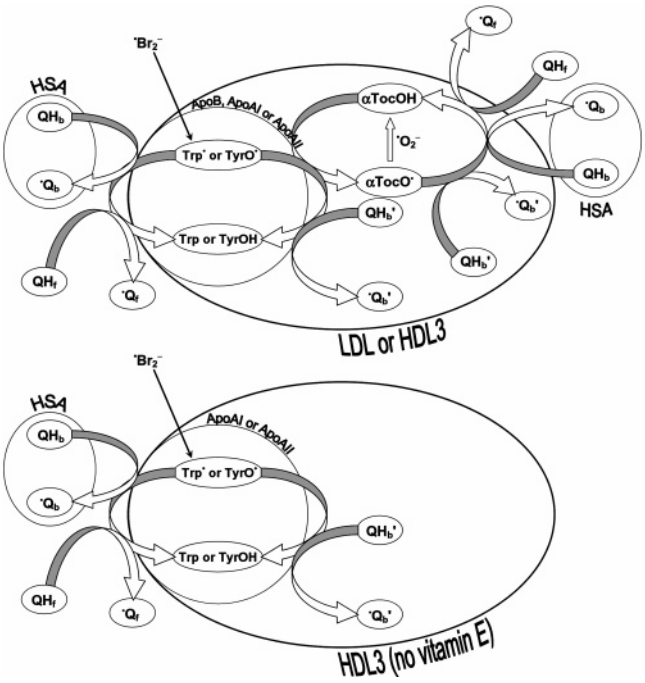

FIGURE 6: Scheme illustrating the sequence of reactions beginning with the oxidation of Trp and Tyr residues of apolipoproteins followed by repair of the phenoxyl Tyr radical by α-tocopherol. Subsequent partial repair of all the radical species by free and HSA-bound quercetin is shown. For HDL_3 in which α-tocopherol is absent, apolipoprotein radicals can be repaired by free and HSA-bound quercetin.

provides an exemplary tool for characterizing the multiplicity of electron transfer processes involved in lipoprotein oxidation and mechanisms of repair in physiological systems.

ACKNOWLEDGMENT

The authors wish to thank M.-A. Conte for her preparation of HDL_3 and LDL. P.F. thanks the "Sociedade Portugesa de Dermatologia e Venerologia" for a travel grant.

REFERENCES

1. Steinbrecher, U. P., Zhang, H. F., and Lougheed, M. (1990) Role of oxidatively modified LDL in atherosclerosis, *Free Radical Biol. Med. 9*, 155−168.
2. Mattson, M. P., Duan, W., Pedersen, W. A., and Culmsee, C. (2001) Neurodegenerative disorders and ischemic brain diseases, *Apoptosis 6*, 69−81.
3. Davies, K. J. (1987) Protein damage and degradation by oxygen radicals. I. General aspects, *J. Biol. Chem. 262*, 9895−9901.
4. Hawkins, C. L., Pattison, D. I., and Davies, M. J. (2003) Hypochlorite-induced oxidation of amino acids, peptides and proteins, *Amino Acids 25*, 259−274.
5. Salmon, S., Mazière, J.-C., Santus, R., Morlière, P., and Bouchemal, N. (1990) UVB-induced photoperoxidation of lipids of human low and high density lipoproteins. A possible role of tryptophan residues, *Photochem. Photobiol. 52*, 541−545.
6. Goldstein, J. L., and Brown, M. S. (1977) The low-density lipoprotein pathway and its relation to atherosclerosis, *Annu. Rev. Biochem. 46*, 897−930.
7. Zheng, L., Settle, M., Brubaker, G., Schmitt, D., Hazen, S. L., Smith, J. D., and Kinter, M. (2005) Localization of nitration and chlorination sites on apolipoprotein A-I catalyzed by myeloperoxidase in human atheroma and associated oxidative impairment in ABCA1-dependent cholesterol efflux from macrophages, *J. Biol. Chem. 280*, 38−47.
8. Parthasarathy, S., Barnett, J., and Fong, L. G. (1990) High-density lipoprotein inhibits the oxidative modification of low-density lipoprotein, *Biochim. Biophys. Acta 1044*, 275−283.
9. Babior, B. M. (1978) Oxygen-dependent microbial killing by phagocytes (first of two parts), *N. Engl. J. Med. 298*, 659−668.
10. Ghibaudi, E., and Laurenti, E. (2003) Unraveling the catalytic mechanism of lactoperoxidase and myeloperoxidase, *Eur. J. Biochem. 270*, 4403−4412.
11. Francis, G. A., Mendez, A. J., Bierman, E. L., and Heinecke, J. W. (1993) Oxidative tyrosylation of high density lipoprotein by peroxidase enhances cholesterol removal from cultured fibroblasts and macrophage foam cells, *Proc. Natl. Acad. Sci. U.S.A. 90*, 6631−6635.
12. Solar, S., Solar, W., and Getoff, N. (1984) Resolved multisite OH-attack on aqueous tryptophan studied by pulse radiolysis, *Radiat. Phys. Chem. 23*, 371−376.
13. Peng, D.-Q., Wu, Z., Brubaker, G., Zheng, L., Settle, M., Gross, E., Kinter, M., Hazen, S. L., and Smith, J. D. (2005) Tyrosine modification is not required for myeloperoxidase-induced loss of apolipoprotein A-I functional activities, *J. Biol. Chem. 280*, 33775−33784.
14. Giessauf, A. B., van Wickern, B., Simat, T., Steinhart, H., and Esterbauer, H. (1996) Formation of N-formylkynurenine suggests the involvement of apolipoprotein B-100 centered tryptophan radicals in the initiation of lipid peroxidation, *FEBS Lett. 389*, 136−140.
15. Filipe, P., Morlière, P., Patterson, L. K., Hug, G. L., Mazière, J.-C., Mazière, C., Freitas, J. P., Fernandes, A., and Santus, R. (2002) Repair of amino acid radicals of apolipoprotein B100 of low-density lipoproteins by flavonoids. A pulse radiolysis study with quercetin and rutin, *Biochemistry 41*, 11057−11064.
16. Boullier, A., Mazière, J.-C., Filipe, P., Patterson, L. K., Bartels, D. M., Hug, G. L., Freitas, J. P., Santus, R., and Morlière, P. (2007) Interplay of oxygen, vitamin E, and carotenoids in radical reactions following oxidation of Trp and Tyr residues in native HDL_3. Comparison with LDL. A time-resolved spectroscopic analysis, *Biochemistry 46*, 5226−5237.
17. de Whalley, C. V., Rankin, S. M., Hoult, J. R., Jessup, W., and Leake, D. S. (1990) Flavonoids inhibit the oxidative modification of low density lipoproteins by macrophages, *Biochem. Pharmacol. 39*, 1743−1750.
18. Boulton, D. W., Walle, U. K., and Walle, T. (1998) Extensive binding of the bioflavonoid quercetin to human plasma proteins, *J. Pharm. Pharmacol. 50*, 243−249.
19. Havel, R. J., Eder, H. A., and Bragdon, J. H. (1955) The distribution and chemical composition of ultracentrifugally separated lipoproteins in human serum, *J. Clin. Invest. 34*, 1345−1353.
20. Atmeh, R. F., Shepherd, J., and Packard, C. J. (1983) Subpopulations of apolipoprotein A-I in human high-density lipoproteins their metabolic properties and response to drug therapy, *Biochim. Biophys. Acta 751*, 175−188.
21. Filipe, P., Haigle, J., Freitas, J. P., Fernandes, A., Mazière, J.-C., Mazière, C., Santus, R., and Morlière, P. (2002) Anti- and pro-oxidant effects of urate in copper-induced low-density lipoprotein oxidation, *Eur. J. Biochem. 269*, 5474−5483.
22. Sowell, A. L., Huff, D. L., Yeager, P. R., Caudill, S. P., and Gunter, E. W. (1994) Retinol, α-tocopherol, lutein/zeaxanthin, α-cryptoxanthin, lycopene, α-carotene, trans-β-carotene, and four retinyl esters in serum determined simultaneously by reversed-phase HPLC with multiwavelength detection, *Clin. Chem. 40*, 411−416.
23. Aksnes, L. (1994) Simultaneous determination of retinol, alpha-tocopherol, and 25-hydroxyvitamin D in human serum by high performance liquid chromatography, *J. Pediatr. Gastroenterol. Nutr. 18*, 339−343.
24. Thurnham, D. I., Smith, E., and Flora, P. S. (1988) Concurrent liquid-chromatography assay of retinol, α-tocopherol, β-carotene, α-carotene, lycopene and β-cryptoxanthin in plasma, with tocopherol acetate as internal standard, *Clin. Chem. 34*, 377−381.
25. Dufour, C., and Dangles, O. (2005) Flavonoid-serum albumin complexation: determination of binding constants and binding sites by fluorescence spectroscopy, *Biochim. Biophys. Acta 1721*, 164−173.
26. Patterson, L. K., and Lilie, J. A. (1974) Computer-controlled pulse radiolysis system, *Int. J. Radiat. Phys. Chem. 6*, 129−141.
27. Hug, G. L., Wang, Y., Schoneich, C., Jiang, P. Y., and Fessenden, R. W. (1999) Multiple time scale in pulse radiolysis: applications to bromide solutions and dipeptides, *Radiat. Phys. Chem. 54*, 559−566.
28. Schuler, R. H., Patterson, L. K., and Janata, E. (1980) Yield for the scavenging of OH radicals in the radiolysis of N_2O-saturated aqueous solutions, *J. Phys. Chem. 84*, 2088−2089.
29. Filipe, P., Morlière, P., Patterson, L. K., Hug, G. L., Mazière, J.-C., Freitas, J. P., Fernandes, A., and Santus, R. (2004) Oxygen-copper (II) interplay in the repair of semi-oxidized urate by quercetin bound to human serum albumin, *Free Radical Res. 38*, 295−301.
30. Manach, C., Morand, C., Texier, O., Favier, M. L., Agullo, G., Demigné, C., Régérat, F., and Rémésy, C. (1995) Quercetin metabolites in plasma of rats fed diets containing rutin or quercetin, *J. Nutr. 125*, 1911−1922.
31. Farhataziz, and Ross, A. B. (1977) Selected specific rates of reactions of transients from water in aqueous solutions. III. Hydroxyl radical and perhydroxyl radical and their radical ions, *NSRDS-NBS 59*.
32. Davies, M. J., Forni, L. G., and Wilson, R. L. (1988) Vitamin E analogue Trolox C. E.S.R. and pulse-radiolysis studies of free-radical reactions, *Biochem. J. 255*, 513−522.
33. Jovanovic, S. V., Steenken, S., Simic, M. G., and Hara, Y. (1998) Antioxidant properties of flavonoids: reduction potentials and electronic transfer reactions of flavonoid radicals, in *Flavonoids in Health and Disease* (Rice-Evans, C., and Packer, L., Eds.), pp 137−161, Marcel Dekker, New York.
34. Filipe, P., Morlière, P., Patterson, L. K., Hug, G. L., Mazière, J.-C., Mazière, C., Freitas, J. P., Fernandes, A., and Santus, R. (2002) Mechanisms of flavonoid repair reactions with amino acid radicals in models of biological systems: a pulse radiolysis study in micelles and human serum albumin, *Biochim. Biophys. Acta 1572*, 150−162.
35. Jovanovic, S. V., Steenken, S., Tosic, M., Marjanovic, B., and Simic, M. G. (1994) Flavonoids as antioxidants, *J. Am. Chem. Soc. 116*, 4846−4851.
36. Noguchi, N., and Niki, E. (1998) Dynamics of vitamin E action against LDL oxidation, *Free Radical Res. 28*, 561−572.
37. Mullen, W., Edwards, C. A., and Crozier, A. (2006) Absorption, excretion and metabolite profiling of methyl-, glucuronyl-, glucosyl and sulpho-conjugates of quercetin in human plasma and urine after ingestion of onions, *Br. J. Nutr. 96*, 107−116.

38. Manach, C., Morand, C., Crespy, V., Demigné, C., Texier, O., Régérat, F., and Rémésy, C. (1998) Quercetin is recovered in human plasma as conjugated derivatives which retain antioxidant properties, *FEBS Lett. 426*, 331−336.
39. Janisch, K. M., Williamson, G., Needs, P., and Plumb, G. W. (2004) Properties of quercetin conjugates: modulation of LDL oxidation and binding to human serum albumin, *Free Radical Res. 38*, 877−884.
40. Cadenas, E., Merényi, G., and Lind, J. (1989) Pulse radiolysis study on the reactivity of Trolox C phenoxyl radical with superoxide anion, *FEBS Lett. 253*, 235−238.
41. Reyftmann, J.-P., Santus, R., Mazière, J.-C., Morlière, P., Salmon, S., Candide, C., Mazière, C., and Haigle, J. (1990) Sensitivity of tryptophan and related compound to oxidation induced by lipid autoperoxidation. Application to human serum low and high density lipoproteins, *Biochim. Biophys. Acta 1042*, 159−167.
42. Kalyanaraman, B., Darley-Usmar, V., Struck, A., Hogg, N., and Parthasarathy, S. (1995) Role of apolipoprotein B-derived radical and alpha-tocopheroxyl radical in peroxidase-dependent oxidation of low density lipoprotein, *J. Lipid Res. 36*, 1037−1045.
43. Rice-Evans, C. A., Miller, N. J., and Paganga, G. (1996) Structure-antioxidant activity relationships of flavonoids and phenolic acids, *Free Radical Biol. Med. 20*, 933−956.
44. Mayer, B., Schumacher, M., Brandstatter, H., Wagner, F. S., and Hermetter, A. (2001) High-throughput fluorescence screening of antioxidative capacity in human serum, *Anal. Biochem. 297*, 144−153.

BI701419D